Ferro- and antiferromagnetic interactions in face-sharing trioctahedral $Ni^{II}Mn^{II}Ni^{II}$ and $Ni^{II}Fe^{III}Ni^{II}$ complexes with the same 1–5/2–1 spin system†

Tamami Kobayashi,[a] Tomoka Yamaguchi,[a] Hiromi Ohta,[a] Yukinari Sunatsuki,[a] Masaaki Kojima,*[a] Nazzareno Re,[b] Matsuo Nonoyama[c] and Naohide Matsumoto[d]

Received (in Cambridge, UK) 12th December 2005, Accepted 17th March 2006
First published as an Advance Article on the web 10th April 2006
DOI: 10.1039/b517503h

Two heterotrinuclear complexes, $[Mn^{II}(Ni^{II}L)_2]\cdot 2CH_3OH$ (where H_3L = 1,1,1-tris(*N*-salicylideneaminomethyl)ethane) and $[Fe^{III}(Ni^{II}L)_2]NO_3\cdot C_2H_5OH$, consisting of three face-sharing octahedra have been prepared; although these complexes have closely related structures and have the same 1–5/2–1 spin system, they show completely different magnetic interactions between the adjacent metal ions: ferromagnetic (Ni^{II}–Mn^{II}) and antiferromagnetic (Ni^{II}–Fe^{III}).

The magnetic properties of multinuclear 3d metal complexes have fascinated researchers for over a half a century. As a result of an enormous volume of study, we can predict the magnetic properties of many complexes from knowing their molecular structures; we have now almost come to the point where we can design a complex molecule with a desired magnetic property.[1] Among the large number of 3d multinuclear complexes, the number of triply bridged face-sharing complexes is small[2] compared with the number of doubly bridged edge-sharing complexes. This is mainly due to the difficulty in designing their ligand system, and the magnetostructural relationships that exist are still not clear. Face-sharing multinuclear complex systems are of importance in understanding overlapping magnetic orbitals, since both $d_{x^2-y^2}$ and d_{z^2} orbitals are concerned with bridging. By employing a "complexes as ligands" strategy,[3] we have prepared two face-sharing linear trinuclear complexes, $Ni^{II}Mn^{II}Ni^{II}$ and $Ni^{II}Fe^{III}Ni^{II}$. A mononuclear Ni^{II} complex, $[Ni^{II}L]^-$, coordinates to the central Mn^{II} or Fe^{III} ion through three bridging phenolate oxygen atoms, where L^{3-} denotes the tripodal hexadentate Schiff base-phenolate ligand (H_3L = 1,1,1-tris(*N*-salicylideneaminomethyl)ethane; Fig. 1(a)). The two complexes have closely related crystal structures and exhibit the same 1–5/2–1 spin system; therefore, we naturally expected that they would exhibit similar magnetic interactions. However, their magnetic interactions are different, being ferromagnetic and antiferromagnetic between the adjacent metal ions, in the Mn^{II} and Fe^{III} systems, respectively. Thus, this system provides a unique opportunity to develop a better understanding of overlapping magnetic orbitals. To the best of our knowledge, such a system has not been reported on so far even in the dinuclear Ni–M (M = Mn^{II}, Fe^{III}) system. Here, we report on the synthesis, crystal structure, and magnetic properties of the two complexes.

The orange complex, $[Mn^{II}(Ni^{II}L)_2]\cdot 2CH_3OH$ (**1**), was prepared using the reaction of [Ni(HL)] and $MnCl_2\cdot 4H_2O$ in methanol in a 2 : 1 mole ratio, with the addition of triethylamine (2 equiv.) to deprotonate the HL^{2-} ligand. The dark purple complex, $[Fe^{III}(Ni^{II}L)_2]NO_3\cdot C_2H_5OH$ (**2**), was prepared in a similar manner. The [Ni(HL)] was allowed to react with $Fe(NO_3)_3\cdot 9H_2O$ and triethylamine in ethanol in a 2 : 1 : 2 mole ratio. The crystal structures of **1** and **2** were determined using single-crystal X-ray diffraction analysis.‡ Figs. 1(b) and 1(c) show the molecular structure of **1** and a view of the $N_3Ni(\mu\text{-}O)_3Mn(\mu\text{-}O)_3NiN_3$ core, respectively. The overall structure is similar to that of the homonuclear Ni^{II} complex, $[Ni^{II}(Ni^{II}L)_2]$.[4] Complex **1** contains two octahedral Ni^{II} ions, and each ion is coordinated by the hexadentate L^{3-} ligand with a facial N_3O_3 donor set. Each $[NiL]^-$ unit caps the Mn^{II} ion *via* three bridging phenolate oxygen donor atoms. The complex is linear, with the Ni···Mn distance being 2.92085(11) Å, and the Ni···Ni distance being 5.8400(9) Å. The average Ni–O–Mn bond angle is 86.6(4)°, and the Ni···Mn···Ni angle is 177.23(2)°. The aromatic rings are stacked with an average distance between the paired rings of *ca.* 3.5 Å. The structure of **2** is very similar to that of **1**. The average Ni···Fe distance is 2.8154(4) Å, and the Ni···Ni distance is 5.6308(6) Å. The average Ni–O–Fe bond angle is 86.2(7)°, and the Ni···Fe···Ni angle is 180.00(11)°. Compounds **1** and **2** are discrete molecules, with the shortest intermolecular metal–metal distance being 9.6318(9) Å in **1** and 9.5394(3) Å in **2**.

Temperature-dependent molar susceptibility measurements on powdered samples of **1** and **2** were carried out in an applied field of 0.1 T in the temperature range 1.9–300 K. The data are shown in the $\chi_M T$ *versus* T plot in Fig. 2, where χ_M is the molar magnetic susceptibility and T is the absolute temperature. The value of $\chi_M T$ of compound **1** is $\chi_M T$ = 7.04 cm^3 K mol^{-1} at 300 K, and this value increases with decreasing temperature, and reaches a maximum of $\chi_M T$ = 13.29 cm^3 K mol^{-1} at T = 7.0 K. The value of $\chi_M T$ then drops sharply. The magnetic behavior of **2** is completely different from that of **1**, although both complexes have the same spin system, 1–5/2–1. The value of $\chi_M T$ for **2** is $\chi_M T$ = 6.56 cm^3 K mol^{-1} at 300 K, and $\chi_M T$ decreases smoothly with

[a]*Department of Chemistry, Faculty of Science, Okayama University, Tsushima-naka 3-1-1, Okayama 700-8530, Japan. E-mail: kojima@cc.okayama-u.ac.jp; Fax: +81-86-251-7842*
[b]*Facolta di Farmacià, Universita degli Studi "G. D'Annunzio", I-66100 Chieti, Italy*
[c]*Department of Chemistry, Faculty of Science, Nagoya University, Chikusa, Nagoya 464-8602, Japan*
[d]*Department of Chemistry, Faculty of Science, Kumamoto University, Kumamoto 860-8555, Japan*

† Electronic supplementary information (ESI) available: Synthesis and characterization of **1** and **2**, X-ray molecular structure of **2**, and the field dependence of magnetization of **2** at 1.9 K. See DOI: 10.1039/b517503h

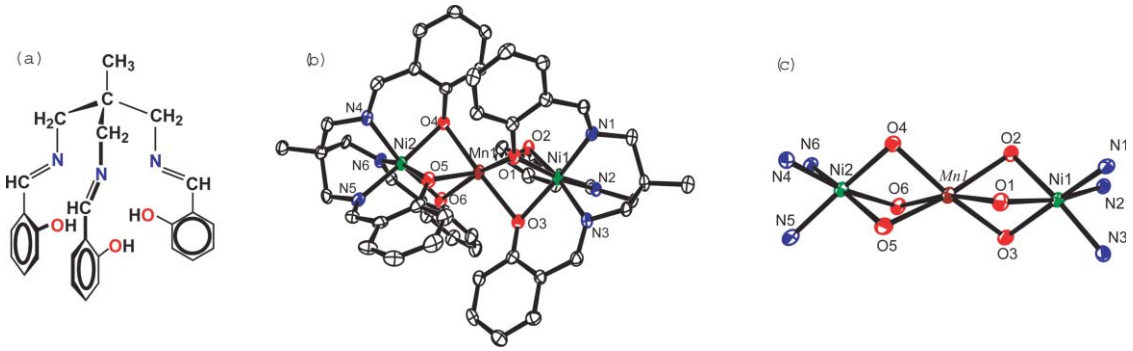

Fig. 1 The structure of the H_3L ligand (a), the molecular structure of $[Mn^{II}(Ni^{II}L)_2]$ (**1**) (b), and a view of the $N_3Ni(\mu\text{-}O)_3Mn(\mu\text{-}O)_3NiN_3$ core of **1** (c).

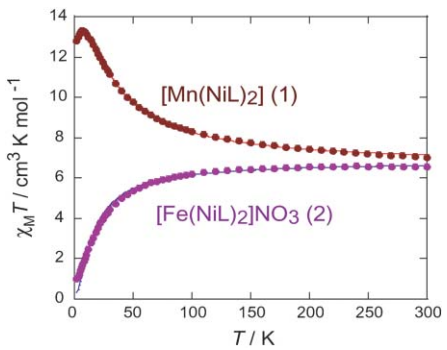

Fig. 2 Magnetic behavior of **1** and **2** in the form of the $\chi_M T$ *vs.* T plots; the solid lines correspond to the best data fits (*cf.* text).

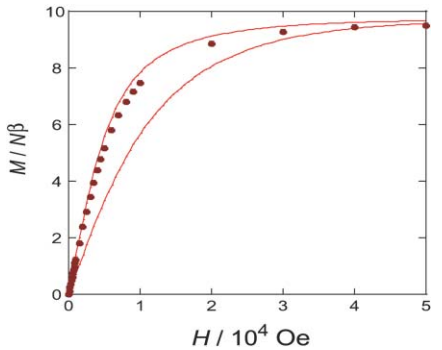

Fig. 3 Field dependence of magnetization at 1.9 K for **1**. The lower solid line corresponds to the non-interacting metal ions, and the upper solid line is the calculated Brillouin curve for $S = 9/2$ with $g_{av} = 2.16$ (*cf.* text).

decreasing temperature. The profiles of the $\chi_M T$ *versus* T curves indicate that the overall magnetic interactions between the metal ions are ferromagnetic ($S = 9/2$ in the ground state) in **1**, while those in **2** are antiferromagnetic ($S = 1/2$ in the ground state). The spin Hamiltonian in linear trinuclear complexes is given by $H = -2(J_{12}S_1 \cdot S_2 + J_{23}S_2 \cdot S_3 + J_{13}S_1 \cdot S_3)$, where $S_1 = S_3 = 1$ and $S_2 = 5/2$ for the S_1–S_2–S_3 arrangement. The terminal Ni^{II} ions are nearly equivalent for **1**, and those for **2** are crystallographically equivalent. Thus, the spin exchange coupling constant for the interactions between the adjacent ions is expressed as $J_{12} = J_{23}$. Fits to the experimental data were carried out, including a zero field splitting (ZFS) term for Ni^{II}. The best fit parameters to the data for **1** were g(Ni) = 2.29, g(Mn) = 1.91, J(Ni–Mn) = +4.65 cm^{-1}, and D(Ni) = −1.75 cm^{-1}. There is no coupling between the two terminal Ni^{II} ions, *i.e.*, J(Ni–Ni) = 0 cm^{-1}. Ferromagnetic interactions between the terminal Ni^{II} ion and the central M^{II} ion have been observed in the same type of LNi^{II}–M^{II}–$Ni^{II}L$ complexes (where M = Ni,[4] Co[5]). For **2**, using a value of g(Ni) = 2.29 from the data fit of **1**, and neglecting D(Ni), which is justified because its effect is strongly coupled with that of the negative value of J, we obtained g(Ni) = 2.29 (fixed), g(Fe) = 1.97, and $J = -1.85$ cm^{-1}.

The field dependence of the magnetization at 1.9 K was also measured, and the M *versus* H curve for **1** is shown in Fig. 3. The saturation magnetization of 9.5 $N\beta$ is observed at 5 T, and the value corresponds fairly well with 9 $N\beta$ expected for the ferromagnetic system. The data are reproduced by a Brillouin curve[1] for $S = 9/2$ with $g_{av} = 2.16$ and the ferromagnetic interaction is confirmed.

It should be noted that complexes **1** and **2** show completely different magnetic exchange interactions, although they have the same 1–5/2–1 spin system and have similar crystal structures. A qualitative interpretation of the magnetic exchange between the two metal centers may be given using Goodenough–Kanamori rules[6] based on the relevant ferromagnetic (orthogonal) and antiferromagnetic (superexchange) pathways. As both Ni^{II} and the central metal ions are in an octahedral environment, the d^8 Ni^{II} center has two magnetic orbitals with e_g (d_{z^2} and $d_{x^2-y^2}$) symmetry, while the high spin d^5 Mn^{II} or Fe^{III} center has five magnetic orbitals with both t_{2g} (d_{xy}, d_{xz}, and d_{yz}) and e_g (d_{z^2} and $d_{x^2-y^2}$) symmetry (Scheme 1). Therefore, both orthogonal, t_{2g}–e_g, and superexchange, e_g–e_g, pathways are possible between adjacent metal ions and, as the latter is known to prevail, a weak antiferromagnetic coupling is expected in both **1** and **2**. In the manganese complex **1**, a small ferromagnetic coupling was observed, suggesting that the Mn–Ni superexchange overlap is weaker than the Fe–Ni overlap. The reason for this weaker antiferromagnetic contribution in **1** is attributed to the small

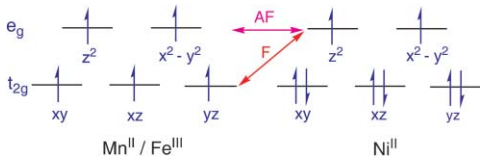

Scheme 1 Electron configurations for Ni^{II} and M^{II} (M = Mn, Fe) ions in an octahedral coordination environment showing the magnetic orbitals.

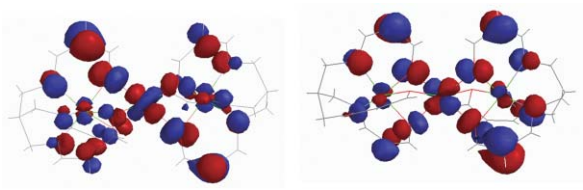

Fig. 4 Two magnetic orbitals representing the main superexchange pathways in compound **2**. Similar magnetic orbitals are calculated for **1**, but with a minor contribution on the bridging oxygen atoms.

structural difference from **2** and, in particular, to the longer Mn–O bond distances (2.15–2.21 Å) compared with the Fe–O bond distances (2.01–2.02 Å). Indeed, experimental[7] and theoretical[8] studies have shown that the antiferromagnetic coupling between oxo- and hydroxo-bridged Fe(III) dinuclear complexes strongly decreases with the lengthening of the Fe–O bond distance. The Ni–O–M bridging angles, a major factor influencing the superexchange interactions, are almost the same for the two complexes as described above.

To better understand the reason for the different magnetic behavior of complexes **1** and **2**, we undertook a theoretical study using methods based on density functional theory. The hybrid B3LYP functional was used in all our calculations, as implemented in the Gaussian03 program. This functional provides excellent results for the calculation of the exchange coupling in a wide range of transition metal complexes.[8–10] We employed an all-electron 6-31G* basis set for the metal and other elements. We considered a slightly simplified model, in which the benzene groups in the tripodal ligand, L^{3-}, were replaced by ethylene moieties with geometries taken from the X-ray crystallographic data. We used the broken symmetry (BS) approach, through which the superexchange coupling constant, J, in the Hamiltonian, $H = -2J(S_1 \cdot S_2 + S_2 \cdot S_1)$, employed in the fitting discussed above, was evaluated using the energy of the highest-spin state, E_{HS}, and the broken symmetry state, E_{BS}, corresponding to the spin flip of the central metal atom using the equation, $E_{HS} - E_{BS} = -2(2S_1S_2 + S_2)J = -30J$.[10a] The calculated coupling constants for **1** and **2** are +11.2 and −19.7 cm^{-1}, respectively, which are in reasonable qualitative agreement with the experimental values, especially with regards to the ferro (+) or antiferromagnetic (−) sign. Fig. 4 shows two selected molecular magnetic orbitals from the high spin calculations of compound **2**. These molecular magnetic orbitals are composed of the local magnetic orbitals on each paramagnetic metal ion, and the selected orbitals show the most effective antiferromagnetic superexchange e_g–e_g pathway. Similar magnetic orbitals were calculated for **1**, but with a minor contribution of the bridging oxygen atoms (see below).

To study the influence of the M–O bond distance (where M = Mn and Fe) on the magnetic exchange, we calculated the Mulliken overlap population, P_{MO}, and the Mulliken spin overlap population, P^S_{MO}, which describe the degree of interaction between M and O atoms and have been recently reported to correlate with the antiferromagnetic coupling constant in Fe^{III} and Cu^{II} oxo-bridged dinuclear compounds.[8,10b] The calculated values were $P_{FeO} = 0.43$ and $P_{MnO} = 0.35$, and $P^S_{FeO} = 0.11$ and $P^S_{MnO} = 0.07$, respectively, which suggest a lower superexchange antiferromagnetic interaction through the bridging oxygen atom in **1** with respect to **2**.

This study has shown that, by the reaction of $[Ni^{II}L]^-$ with Mn^{II} and Fe^{III}, linear trinuclear complexes $[Mn^{II}(Ni^{II}L)_2]$ (**1**) and $[Fe^{III}(Ni^{II}L)_2]^+$ (**2**) were formed, respectively. Although both complexes have the same 1–5/2–1 spin system and closely related crystal structures, temperature-dependent magnetic susceptibility measurements revealed that **1** has an $S = 9/2$ ground state whereas **2** has an $S = 1/2$ ground state. Theoretical studies have confirmed that the different magnetic behavior is attributable to the small difference in M–O bond distance.

This work was supported in part by a Grant-in-Aid for Scientific Research (Nos. 16205010, 16750050, and 17350028) from the Ministry of Education, Science, Sports, and Culture of Japan, and by the Iketani Science and Technology Foundation. T. Y. was supported by JSPS program for Research Fellowships for Young Scientists (No. 17003601).

Notes and references

‡ Crystal data for **1**: $C_{53}H_{52}N_6Ni_2MnO_7$, $M = 1057.37$, monoclinic, space group $P2_1/n$ (no. 14), $a = 16.3186(8)$, $b = 16.1878(1)$, $c = 18.4263(1)$ Å, $\beta = 108.443(3)^\circ$, $V = 4617.5(5)$ Å^3, $Z = 4$, $F(000) = 2196.00$, $D_c = 1.521$ g cm^{-3}, $\lambda = 0.71069$ Å, $T = -150 \pm 1$ °C, μ(Mo-Kα) = 11.389 cm^{-1}, 27255 reflections measured, 9012 unique ($R_{int} = 0.060$), $R1 = 0.0648$ ($I > 2.0\sigma(I)$), w$R2 = 0.1630$. CCDC 293099.

Crystal data for **2**: $C_{58}H_{72}FeN_7Ni_2O_{15}$ $M = 1280.49$, monoclinic, space group $P2_1/c$ (no. 14), $a = 13.6537(6)$, $b = 11.6810(4)$, $c = 18.7123(5)$ Å, $\beta = 103.8870(2)^\circ$, $V = 2897.17(2)$ Å^3, $Z = 2$, $F(000) = 1342.00$, $D_c = 1.468$ g cm^{-3}, $\lambda = 0.71069$ Å, $T = -150 \pm 1$ °C, μ(Mo-Kα) = 9.640 cm^{-1}, 20995 reflections measured, 6397 unique ($R_{int} = 0.047$), $R1 = 0.0469$ ($I > 2.0\sigma(I)$), w$R2 = 0.1225$. CCDC 293098. In **2** a nitrate ion is disordered about an inversion center and we were unable to generate a physically reasonable model for it.

For crystallographic data in CIF or other electronic format see DOI: 10.1039/b517503h

1 O. Kahn, *Molecular Magnetism*, VCH, Weinheim, 1993.
2 (*a*) A. P. Ginsberg, R. L. Martin and R. C. Sherwood, *Inorg. Chem.*, 1968, **7**, 932; (*b*) P. D. W. Boyd and R. L. Martin, *J. Chem. Soc., Dalton Trans.*, 1979, 92; (*c*) P. Chaudhuri, M. Winter, B. P. C. Della Vedova, P. Fleischauer, W. Haase, U. Florke and H.-J. Haupt, *Inorg. Chem.*, 1991, **30**, 4777; (*d*) T. Beissel, F. Birkelbach, E. Bill, T. Glaser, F. Kesting, C. Krebs, T. Weyhermüller, K. Wieghardt, C. Butzlaff and A. F. Trautwein, *J. Am. Chem. Soc.*, 1996, **118**, 12376; (*e*) Y. Garcia, P. Guionneau, G. Bravic, D. Chasseau, J. A. K. Howard, O. Kahn, V. Ksenofontov, S. Reiman and P. Gütlich, *Eur. J. Inorg. Chem.*, 2000, 1531; (*f*) T. Glaser, F. Kesting, T. Beissel, E. Bill, T. Weyhermüller, W. Meyer-Klaucke and K. Wieghardt, *Inorg. Chem.*, 1999, **38**, 722; (*g*) U. Auerbach, C. Stockheim, T. Weyhermüller, K. Wieghardt and B. Nuber, *Angew. Chem., Int. Ed. Engl.*, 1993, **32**, 714.
3 T. Yamaguchi, Y. Sunatsuki, M. Kojima, H. Akashi, M. Tsuchimoto, N. Re, S. Osa and N. Matsumoto, *Chem. Commun.*, 2004, 1048.
4 H. Ohta, K. Harada, K. Irie, S. Kashino, T. Kambe, G. Sakane, T. Shibahara, S. Takamizawa, W. Mori, M. Nonoyama, M. Hirotsu and M. Kojima, *Chem. Lett.*, 2001, 842.
5 T. Kobayashi, T. Yamaguchi, H. Ohta, Y. Sunatsuki, M. Kojima, N. Re and N. Matsumoto, unpublished work.
6 (*a*) J. B. Goodenough, *Phys. Rev.*, 1955, **100**, 564; (*b*) J. Kanamori, *J. Phys. Chem. Solids*, 1959, **10**, 87.
7 (*a*) D. M. Kurtz, Jr., *Chem. Rev.*, 1990, **90**, 585; (*b*) G. Haselhorst, K. Wieghardt, S. Keller and B. Schrader, *Inorg. Chem.*, 1993, **32**, 520.
8 Z. Chen, Z. Xu, L. Zhang, F. Yan and Z. Lin, *J. Phys. Chem. A*, 2001, **105**, 9710.
9 (*a*) E. Ruiz, J. Cano, S. Alvarez and P. Alemany, *J. Comput. Chem.*, 1999, **20**, 1391; (*b*) E. Ruiz, A. A. Rodríguez-Fortea, J. Cano, S. Alvarez and P. Alemany, *J. Comput. Chem.*, 2003, **24**, 982.
10 (*a*) E. Ruiz, *Struct. Bonding*, 2004, **113**, 71; (*b*) A. Rodríguez-Fortea, P. Alemany, S. Alvarez and E. Ruiz, *Chem.–Eur. J.*, 2001, **7**, 627.

